Automatic Helical Rotorcraft Descent and Landing Using a Microwave Landing System

Leonard A. McGee,* John D. Foster,† and George Xenakis†
NASA Ames Research Center, Moffett Field, California

A helical-approach plan is presented for instrument flight rules operation of rotorcraft into congested terminal areas where separation from high-speed jet traffic is highly desirable and the airport precision-approach aid is a microwave landing system (MLS). The plan takes advantage of the fact that rotorcraft need not land on the main runway but can operate from a pad that lies on an MLS radial offset from the centerline. The results of 49 flights using a UH-1H helicopter and a research avionics system are presented. Four levels of navigation sophistication were also investigated. It is shown that an approach helix can be contained in a relatively small volume and that being within the instrument landing system Category II window at an altitude of 30 m (100 ft) is not a requirement for a successful hover over a landing pad. Only two of the four navigation systems provided estimates that allowed all flights to descend from hover to touchdown.

Introduction

As rotorcraft assume a greater role in the nation's transportation system, the need for rotorcraft instrument flight rule (IFR) operations in high traffic density terminal areas will become more common, aggravating the existing air traffic control problems of mixing low-speed traffic with high-speed jet transport traffic. Yet the efficiency and convenience of the rotorcraft as a feeder to major airports for both corporate and commercial travelers would be diminished if time and fuel were wasted waiting for spacing between arriving and departing jet aircraft. One possible solution to this problem is to separate rotorcraft and jet traffic by assigning them to separate airspaces during approach and landing. With this separation, the problems of aircraft spacing and traffic conflict would be limited to vehicles with similar approach and departure speeds. This scheme could simplify the air traffic control problem and dramatically increase the efficiency of terminal area operations for rotorcraft.

One way to provide aircraft separation is to use a helical approach for the rotorcraft traffic.[1] A helical descent allows the vehicle to lose altitude in a confined airspace without descending along a steep glide slope at very low airspeeds, thus avoiding the poor handling qualities associated with steep rotorcraft descents. The helix can be located in an airspace sector such that it does not conflict with the fixed-wing craft approach and departure corridors in the immediate vicinity of an airport. In the future, it is expected that the primary airport precision approach aid will be the microwave landing system (MLS). If MLS guidance is to be used for such descents at airports that have a single MLS, the helix must be within the lateral and vertical MLS coverage limits, yet displaced sufficiently far from the fixed-wing craft runway to allow simultaneous approaches. To investigate the feasibility of this technique, flight experiments were conducted by using a NASA/Army UH-1H helicopter equipped with a research digital avionics system capable of coupled, automatic approaches to hover and touchdown. These feasibility tests were conducted along a helix tangent to an extension of the runway centerline. Later tests are planned with the helix tangent to a radial offset from the centerline that would achieve the desired separation discussed above.

Four levels of navigation sophistication were evaluated in these flight tests: a Kalman filter using inertial navigation system (INS) platform inertial sensors, a Kalman filter using body-mounted inertial sensors, a complementary filter using body-mounted inertial sensors, and a combination of the INS and complementary filter. The latter combination was flown later with revised software. Pilots' comments from only that flight will be discussed. Hereinafter, these systems will be referred to as the INS-Kalman, the body-Kalman, the body-complementary, and the INS-complementary, respectively. Attitude information used in the guidance and control system was always derived from aircraft vertical and directional gyroscopes.

The objective of this paper is to present flight-test data pertinent to 1) the feasibility of flying helix approaches under IFR conditions, 2) a comparison of the performance of the four levels of navigation sophistication described previously, and 3) the MLS azimuth errors. The feasibility of flying helix approaches is assessed in terms of reference-helix tracking and the resulting airspace required and the dispersions at a decision height of 30 m (100 ft) and at hover. The performances for the different levels of navigation sophistication are measured in terms of the tracking performance, lateral-position errors, dispersions at hover, and pilot comments. These performance measures are only a few of many that must be considered with regard to the feasibility of operating a rotorcraft at an airport concurrently with high-speed jet traffic.

Test Equipment

Test Aircraft

The flight test aircraft was a UH-1H helicopter having a maximum gross weight of 4300 kg and a maximum airspeed of 63 m/s (124 knots) at sea level (see Fig. 1). It is powered by a single, turboshaft T-53-L-13 engine. The flight controls for this aircraft are hydraulically boosted, and rate damping is provided by a gyrobar. The aircraft hydraulic and electrical systems were modified to interface with the research avionics equipment and servoactuators. In addition, special racks for the electronic equipment were installed aft of the pilots' seats. Figure 1 also shows the front and rear MLS receiving antennas. An electronic device automatically monitors the signal strength and switches between the two antennas to present the highest quality signal to the MLS receivers.

Presented as Paper 81-1857 at the AIAA Atmospheric Flight Mechanics Conference, Albuquerque, N.M., Aug. 19-21, 1981; submitted Sept. 30, 1981; revision received Oct. 11, 1983.

*Research Scientist.
†Research Scientist. Member AIAA.

Research Avionics System

The components of the research avionics system[2] are shown in the block diagram in Fig. 2; a brief description of the major components follows.

The central system component is the data adapter, which provides for information transfer between the subsystems. It converts information into the proper signal format for input and output and provides multiplexed analog-to-digital, digital-to-digital, and digital-to-analog conversions.

The vehicle sensors provided measurements of the aircraft attitude, attitude rate, acceleration, and certain air-data parameters such as airspeed, static pressure, and ambient temperature. The airspeed sensor and the static pressure port were located on the end of a 1.4-m boom mounted on the aircraft nose. The boom installation minimized the effects of the main rotor-induced sideslip angles on the true airspeed and static pressure measurements.

The navigation aid data were derived from a radar altimeter and from MLS, Tacan, and VHF omnidirectional range (VOR) receivers. A Litton LTN-51 inertial navigation system provided acceleration data in a local level coordinate frame for the INS-Kalman navigation system. The data-acquisition system collected digital data from the data adapter, converted analog vehicle sensor data to digital data, and sent this combination through a telemetry transmitter to a ground station to be recorded.

The pilot interacted with the research avionics system through the mode select panel, the keyboard, and the multifunction-display control panel. Pilot displays consisted of a conventional electromechanical attitude-director indicator (ADI), a horizontal-situation indicator (HSI), and a cathode-ray tube used as a multifunction display (MFD). The MFD provided position information in a moving-map format so that the pilot could monitor the helical approach by watching a "bug" representing the helicopter and its progress with respect to the described reference path, which was also shown on the display.

The guidance and control laws controlled the aircraft through the servointerlock unit (SIU). This unit contained the hardware necessary to drive the electrohydraulic series servos and the electromechanical parallel servos connected to the aircraft flight controls.

The basic and research 1819B computers are general-purpose, airborne, digital computers that use fixed-point arithmetic. The guidance functions, complementary navigation filter, and control functions, along with routine supporting functions such as display generation and system monitoring, were programmed into the basic computer. Software associated with the Kalman navigation filter was programmed into the research computer.

Test Description

Helical Approach Trajectory

The helical approach trajectory is shown in Fig. 3 along with a 30-m (100-ft) decision-height window and a hover window. The approach begins with a constant-altitude segment 762 m (2500 ft) above ground level (AGL) along the runway centerline extension. The helix, which is flown at 60 knots and at a nominal bank angle of 10 deg, is tangent to this segment at $x = -914$ m (-3000 ft) with a radius of 530 m (1739 ft), where x is the distance to the helipad. The helicopter flight path follows a -6.11 deg glide slope; it originates at the tangent point, goes around the helix twice, and exits from the helix at an altitude of 48.8 m (160 ft), where it rolls out of the turn and heads down the centerline. The approach path follows the -6.11 deg descent until an altitude of 33.7 m (110.6 ft) is reached; it then intercepts a -2.5 deg glide slope originating from the touchdown point. The -2.5 deg glide slope was used to avoid height-velocity combinations that are unsafe under engine failure conditions. The -2.5 deg descent continues past the 30-m (100 ft) decision-height window down to an altitude of 4.6 m (15 ft). The helicopter continues at this altitude until it reaches the hover window over the touchdown point on the runway. The longitudinal velocity along the final segment is controlled by a flare law that initiates a 0.1-g deceleration at the appropriate point so that the velocity at 30 m (100 ft) from the helipad is 5.5 m/s (17.9 ft/s). The velocity is decreased linearly from this point to hover to avoid too great a pitchup maneuver by the helicopter. When the magnitude of the x velocity is less than 0.15 m/s (0.5 ft/s), a letdown is initiated that results in a nominal vertical-touchdown velocity of -0.06 m/s (-0.2 ft/s).

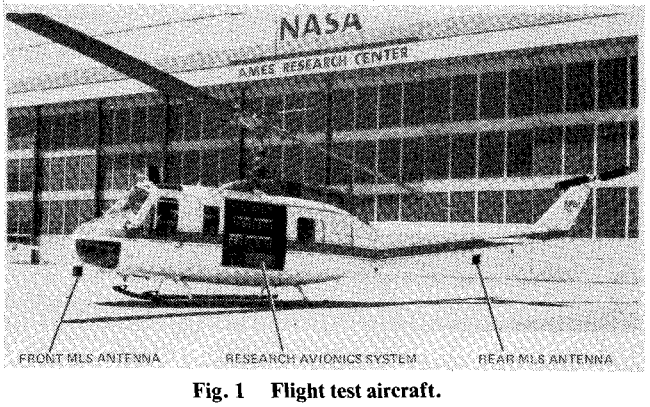

Fig. 1 Flight test aircraft.

Test Procedure

All approaches began with the research avionics system in the automatic heading, altitude, and airspeed-hold modes at an altitude of about 762 m (2500 ft). The pilot steered the aircraft by using the heading-select control to intercept the helix along a course that was parallel to the runway. The aircraft was slowed to an approach speed of 31 m/s (60 knots) at 1.5 km (1 n.mi.) before entering the helix. The automatic system would engage the landing mode when the helicopter was aligned along the runway centerline extension before it entered the helix at a distance of between 2 and 6 km (1 and 3 n.mi.) from the designated touchdown point (see Fig. 3). The approach continued automatically along the helix, along the glide slope to a hover, and finally to touchdown, where the pilot would disconnect the research avionics system and execute a manual takeoff to set up the next approach.

Test Location

The flight tests were conducted at the Naval Auxiliary Landing Field (NALF) at Crows Landing, California, where Ames Research Center has established its Flight Systems Research Facility. Figure 4 shows the facilities at Crows Landing, including the location of the Tacan transmitter, the location of the MLS azimuth and distance measuring equipment (DME) transmitter, and the location of the MLS glide slope transmitting antenna. This is located about midway along runway 35, which has been specially marked to simulate a helipad as well as a short takeoff and landing (STOL) runway. The cross-hatched area is the simulated STOL runway, and the circle represents the helipad. Also shown is the radar tracking facility, which has two radars tracking the helicopter throughout the approach and providing the "actual" position and velocity of the aircraft. This facility maintains time synchronization with the aircraft data via synchronized time-code generators. Test data recorded on the aircraft and transmitted to the tracking facility are merged with the real-time radar tracking data to provide test personnel with a real-time assessment of the navigation, guidance, and control systems on the aircraft. Digital recordings of these merged data are also provided for postflight analysis. The data present in this paper were obtained from the digital recordings.

Radar Tracking Facility Accuracy

The actual position of the aircraft was determined by the radar tracking facility. The accuracy of the radar tracking system was determined using two highly accurate laser trackers as a reference. The results of this evaluation showed radar tracking system 2-σ errors of $\Delta x = 3.7$ m (12 ft), and $\Delta y = \Delta z = 1.2$ m (4 ft) in the STOL touchdown region. No evaluation was done for the touchdown region used for this study. However, it is not expected that the errors would be significantly different from those for the STOL touchdown region.

Navigation, Guidance, and Control Functions

Navigation Functions

The ability of an automatic landing system to follow an approach path requires an estimate of the aircraft position and velocity. Aircraft position measurements with bias errors and high-frequency random noise are common to most state-of-the-art ground navigation aids and associated airborne receivers. The function of the airborne navigation system was to provide estimates of the aircraft position and velocity by using four navigation-filter/inertial-system schemes.

The first and most sophisticated of these utilized a Kalman filter.[3] Inertial accelerations from an LTN-51 inertial navigation system (INS), Tacan range and azimuth readings, and MLS range and azimuth readings were used for horizontal navigation. For vertical navigation, the signals that were used in this Kalman filter were: barometric altitude from a static-pressure sensor, MLS elevation angle, and radar altitude from a radar altimeter. The Kalman filter consisted of two filters, and eight-state horizontal filter and an independent three-state vertical filter. The eight horizontal states were x- and y-position error, x- and y-velocity error, x- and y-acceleration-bias error, the Tacan range bias estimate, and the Tacan bearing bias estimate. Since the INS provided high-quality acceleration data, the acceleration uncertainty modeled in the filter was small. The three vertical states were: z-position estimates, velocity error estimates, and the error in the vertical acceleration bias. When the aircraft was at an altitude greater than 122 m (400 ft) above the ground, the barometric altitude was the primary vertical measurement and the MLS elevation angle was used only to estimate the baro-altitude bias error. For altitudes less than 122 m (400 ft) above the ground, the radar altimeter provided the vertical measurement to the filter.

In the second scheme, a Kalman filter was used that had a structure identical to that of the first filter, with the exception of the LTN-51 INS being replaced by an inertial system that used attitude gyroscopes for the helicopter attitude information and body-mounted accelerometers. These measurements were transformed through the aircraft attitude angles measured by the vertical and directional gyros to give the runway coordinate accelerations that were processed by the filter. These accelerations were subject to greater errors than those measured in the INS platform. Vertical gyro precession during the turns in the helix introduced additional time-varying errors in the computed acceleration. These acceleration errors usually resulted in low-frequency position and velocity estimate errors during the helix segment of the approach. To minimize these errors, the magnitude of acceleration uncertainty modeled in the filter had to be greater than in the previous case in which the accelerations were measured by an INS. In addition to increasing path-tracking dispersions, greater noise in the guidance commands caused greater control activity. Hence, when body-mounted inertial sensors were used, a compromise had to be made between control activity and navigation error. For this flight test program, the modeled uncertainties in the acceleration errors were chosen to minimize control activity, especially when hovering, in order to avoid both lateral and backward motion during touchdown. There was thus some sacrifice of accuracy in the position and velocity estimates during the earlier portion of the approach. A nominal value used for the acceleration uncertainties was 0.1524 m/s^2 (0.5 ft/s^2).

The third scheme involved constant-gain complementary filters, used in place of the Kalman filter to blend the body-mounted inertial sensor data with the Tacan and MLS data.[3] The runway coordinate accelerations were derived from the same sensors and in the same manner as in the second method. In contrast to the other two methods, the filters had

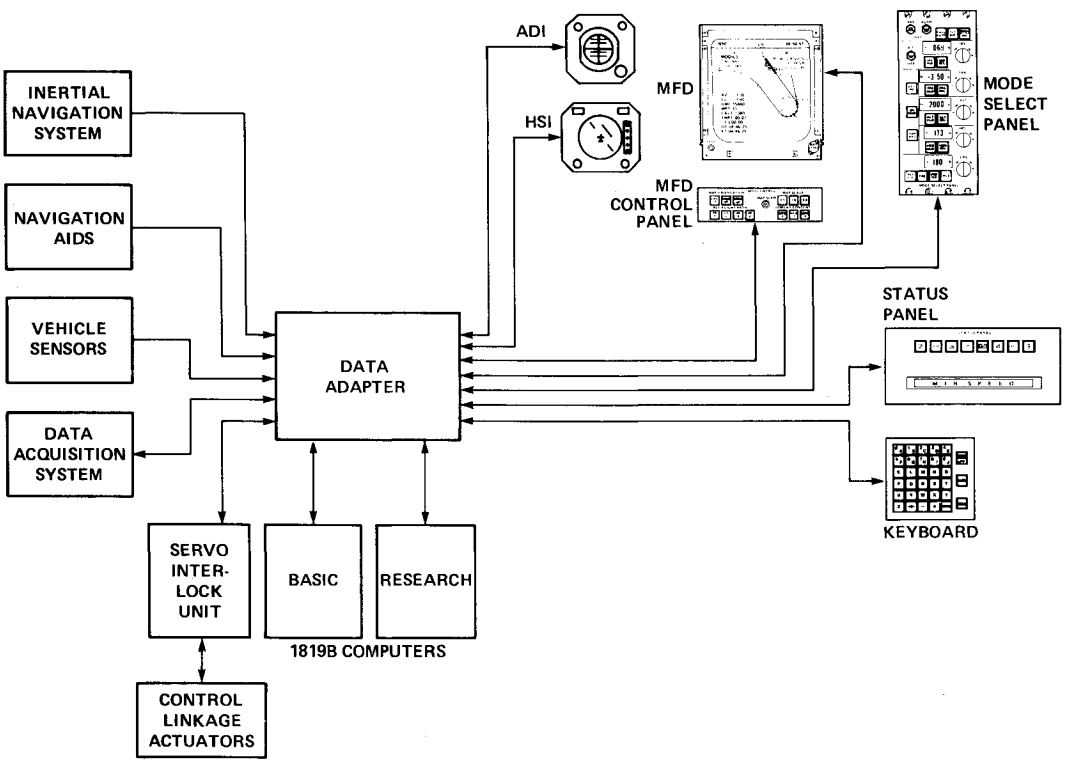

Fig. 2 Components of the research avionics system.[2]

three components that were basically independent. The significant difference between these filters and the Kalman filters was the constancy of measurement gains for a given navigation source, and their invariance with the position relative to that source. There was one set of gains for Tacan measurements and one set for MLS measurements. The gains used for the flight test gave greater sensitivity to high-frequency measurement noise than either of the Kalman filters. Consequently, this filter tended to reduce the effect of the low-frequency inertial errors at the expense of passing more high-frequency measurement noise to the guidance commands. This reduction resulted in greater control activity.

As mentioned previously, the fourth scheme, using the INS-complementary filter, was flown later when the software had been revised. The pilots' comments about this technique will be discussed later.

Guidance Functions

The guidance system had two main functions. One was to use the estimated aircraft position from the navigation system to compute the error from the desired approach flight path that would take the aircraft from an initial approach fix to touchdown at the appropriate airspeeds. The other was to compute aircraft pitch attitude, roll attitude, and vertical speed commands to control the aircraft along the approach flight path without exceeding the aircraft operational limitations. The pilot was able to fly the approach manually or fully automatically, but for this paper only the automatic modes were evaluated. After the pilot selected the automatic modes to be flown, they were implemented automatically upon the occurrence of specific flight conditions. In each case, the pilot was alerted to the mode engaged by an annunciation of the cockpit mode-status panel.

Control Functions

The helicopter controls (longitudinal cyclic, lateral cyclic, collective, and tail rotor blade pitch) were driven by series and parallel servos that moved in response to commands from the stabilization and control equations mechanized in the basic computer of the research avionics system. The series servos were electrohydraulic position servos that produced additive position changes in control linkages that were not reflected in the pilot's stick or pedal positions. The parallel servos were electromechanical rate servos that acted on the stick and pedals to off-load the series servos. Pitch attitude was controlled by the longitudinal cyclic controls, roll attitude by the lateral cyclic controls, and vertical speed by the collective controls. The tail rotor pitch was not controlled by a guidance steering command; it functioned to maintain zero sideslip for airspeeds greater than 19 m/s (37 knots). For speeds less than 19 m/s (37 knots), the tail rotor control maintained aircraft heading.

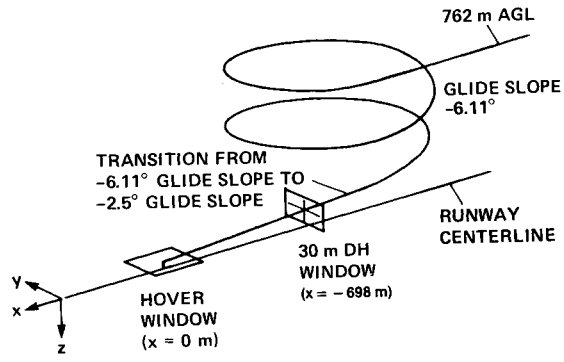

Fig. 3 Helical approach trajectory, including 30-m (100-ft) decision-height window and hover window.

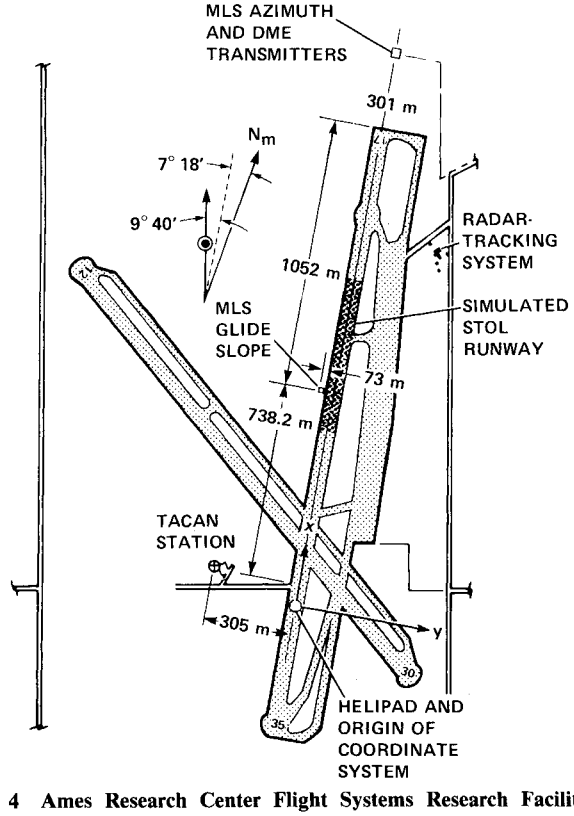

Fig. 4 Ames Research Center Flight Systems Research Facility, NALF, Crows Landing, California.

Results and Discussion

Feasibility of the Helix Approach

Forty-nine automatic helix approaches were completed during the flight tests. In 21 of these, the INS-Kalman navigation system was used, in 14 the body-Kalman navigation system was used, and in 13 the body-complementary navigation system was used. The INS-complementary filter system was used in one approach. The purpose of these flights was, in part, to determine the feasibility of the helix approach by evaluating the airspace requirements and the ability to conduct Category II landings, given an adequate navigation system. The INS-Kalman navigation system was the most accurate of the three systems tested; the flight performance for this system is illustrated in Figs. 5-7.

A composite plot of the helicopter position during the approaches with the INS-Kalman filter is illustrated in Fig. 5. The data for this plot were measured by the ground-based radar tracking facility. The horizontal position plots in the top half of the figure show that the helix part of the approach can be contained in a square of less than 1.2 km (0.65 n.mi.) to a side.

The vertical-position plot in the bottom half of Fig. 5 shows that the altitude dispersions at the top of the helix converge to a small value by the time the helicopter reaches the helix exit. This was true even though the pilot had positioned the helicopter below the capture altitude in several instances. The consistency with which the helicopter arrived at the decision height is illustrated in Fig. 6. Shown are the position, guidance, and navigation errors at a 30-m (100-ft) decision height, which is located 698 m (2290 ft) from the touchdown point. Figure 6a shows the vertical and lateral position errors where "position error" is defined as the difference between the reference and the actual helicopter position measured by a ground-based tracking radar. The solid box is the Category II decision-height window shown in Fig. 3. Figure 6b shows the "guidance error," defined as the difference between the on-

board computation of the reference position and the on board estimate of the position of the helicopter. Figure 6c shows the "navigation error," defined as the difference between the actual position determined from the ground-based radar and the position estimated by the navigation system. The position error is the vector sum of the navigation error and the guidance error. The position error plot shows the tendency for the helicopter to be to the left of the reference flight path at this point. Although not shown, most of the flights with the two body-mounted systems were to the left of the runway centerline.[4] The reason for this will be discussed later.

The guidance error plot also shows the same tendency to be above the reference path; this tendency may be caused by guidance system errors in the transition from the helix descent angle of -6.11 deg to the final -2.5 deg glide slope shown in Fig. 3. The navigation error plot shows very little vertical error, but has a lateral error that averages about -10 m. This error indicated a bias in the navigation system caused by a bias in the output of the MLS azimuth signal receiver. This was later traced to a 0.2 deg bias in the MLS azimuth signal transmission. The effect was that of moving the reference flight path in the negative y-axis direction by 8 m (26 ft) at hover. Although the lateral position error dispersions at the 30-m (100-ft) decision-height window were substantial when compared with the Category II ILS limits, all the approaches were successfully completed to a hover.

Figures 7a and 7b show the longitudinal and lateral aircraft navigation and position dispersions, as measured by the tracking radar about the intended hover point. The solid box in each plot represents the hover window shown in Fig. 3, which is directly above the helipad. The size of the hover window was selected according to FAA guidelines for visual flight rules (VFR) operations of a large transport helicopter.[5] A comparison of Figs. 7a and 7b shows that the position errors bear a significant resemblance to the navigation errors. This similarity occurs because the guidance errors are small at hover.

A comparison of the lateral position at hover shown in Fig. 7b with those at the 30-m (100-ft) decision height shown in Fig. 6 indicates that the automatic approach dispersion criteria limits at the decision height for rotorcraft approaches might be made larger than the Category II limits used for conventional aircraft. Although not shown, all the approaches that were outside the ILS Category II limits at the decision height terminated at hover with acceptable position errors. One major difference between the fixed-wing case, for which the Category II position error limits were specified, and the rotorcraft case is the elapsed time between decision height and touchdown. The helicopter exits the helix at 60 knots and decelerates to a hover from the 30-m (100-ft) decision height in 40 to 50 s. A jet transport would require 15 to 20 s. Thus, there is more time for the helicopter automatic guidance navigation system to reduce the path tracking errors at decision height.

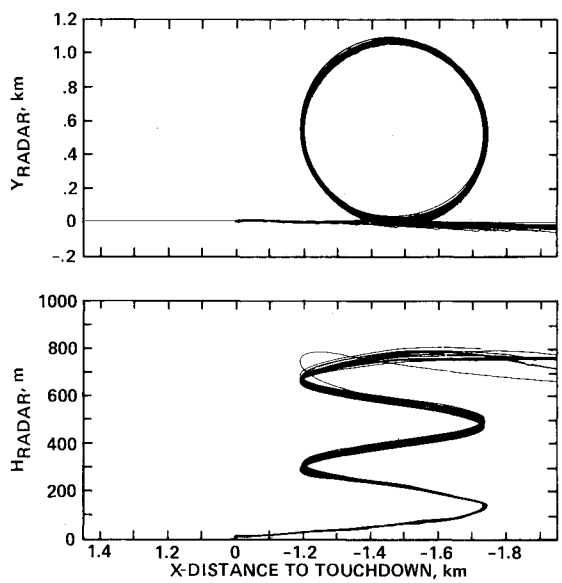

Fig. 5 Composite plot of helicopter position during approaches with INS-Kalman filter.

Comparison of the First Three Navigation Systems

The differences in performance between the first three navigation systems can be seen by comparing Fig. 5 with Figs. 8a and 8b, which show the composite plots for the body-Kalman and body-complementary systems, respectively. The superior performance of the INS-Kalman system is evident, as is the somewhat poorer performance of the body-Kalman system. The deviations from the runway centerline-following helix exit for the body-Kalman and body-complementary

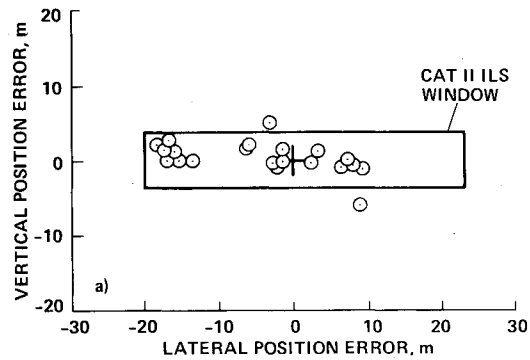

Fig. 6a Vertical and lateral position errors at 30-m (100-ft) decision height 698 m (2290 ft) from touchdown point.

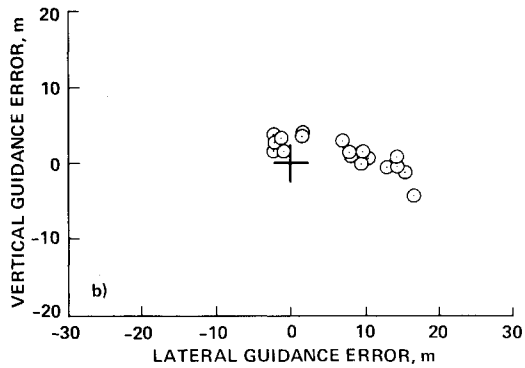

Fig. 6b Guidance error at 30-m (100-ft) decision height 698 m (2290 ft) from touchdown point.

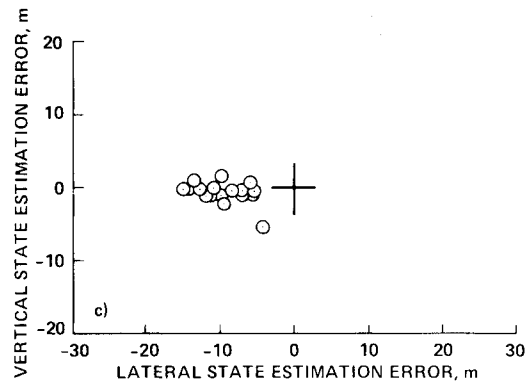

Fig. 6c Navigation error at 30-m (100-ft) decision height 698 m (2290 ft) from touchdown point.

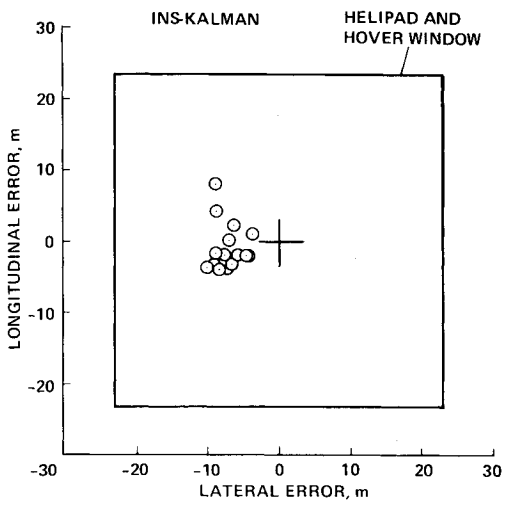

Fig. 7a Longitudinal and lateral aircraft navigation dispersions at hover.

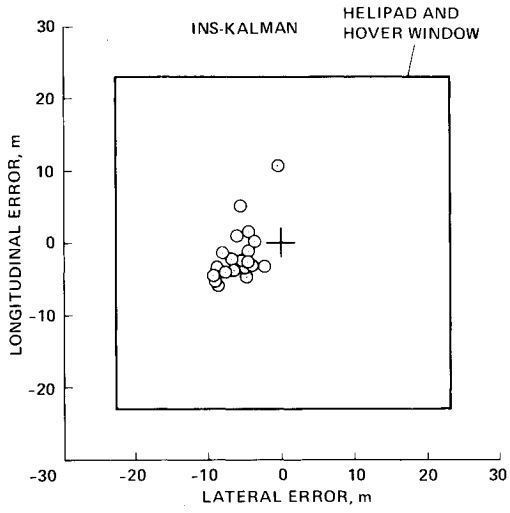

Fig. 7b Longitudinal and lateral aircraft position dispersions at hover.

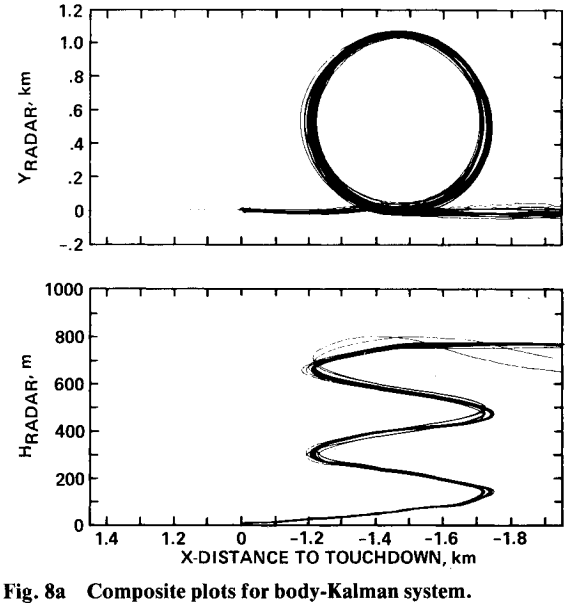

Fig. 8a Composite plots for body-Kalman system.

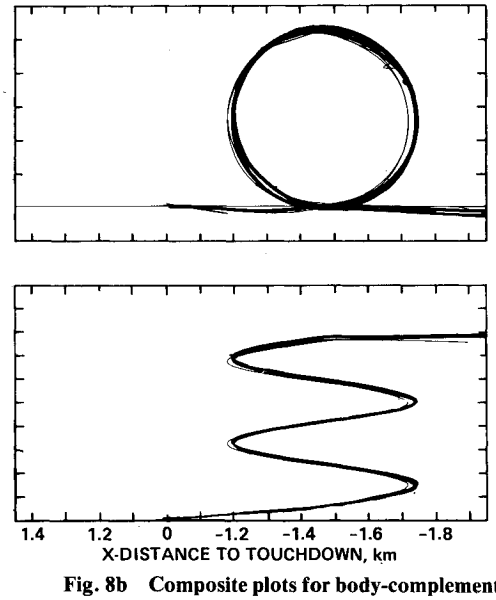

Fig. 8b Composite plots for body-complementary system.

filters, as well as errors in tracking the desired helix, are due mainly to errors in the vertical and directional gyros which measure the aircraft altitudes used to transform the body-derived accelerations into the runway coordinate system. Using the INS as a reference, the pitch, roll, and heading errors had a near-sinusoidal character. The pitch error ranged from about +0.05 to −1.6 deg, ending at hover with an error of +0.04 deg. The roll error ranged from +0.06 to −1.3 deg, settling rapidly to about −0.05 deg after rollout on the final approach. The heading error was more erratic ranging from about +1.6 to −1.8 deg. After rollout on the final approach, the heading error rapidly returned to near-zero with excursions no greater than 0.25 deg after a known bias was removed in the computer. No attempt was made to predict or compensate for attitude errors.

Figure 9 shows the lateral acceleration error as a function of distance to touchdown. The computation of these errors was based on the pitch, roll, and heading error histories described above. This figure shows that the error is negative most of the time because of a small component of gravity remaining after the transformation to the runway coordinate system. The lateral acceleration error also reaches peak values of about 0.27 m/s^2 at distances to touchdown of about 4700 and 1400 m, which correspond to the points where both the pitch and roll errors in the vertical gyro are near a maximum negative error. The effect of these lateral acceleration errors is clearly evident in the next figure.

Figure 10 shows the 2-σ lateral position error envelopes plotted about the mean for the first three navigation systems as functions of the distance to touchdown. The lateral position error is the difference between the reference flight path and the radar-measured helicopter position. For comparison, the FAA 2-σ tracking error limits[6] for a conventional aircraft flying a typical automatic Category II ILS approach are shown as dashed lines in Fig. 10. The discontinuity in the FAA limits results from a decrease in the specification of the error limit maximum sensitivity at a 91-m (300-ft) altitude to a value of about 71% of the initial limits. The limit specification terminates at the 30-m (100-ft) decision height labeled "DH" in the figure.

Figure 10 clearly shows the effect of the lateral acceleration errors shown in Fig. 9 on the lateral position error of the two filters using the body-mounted inertial system. The two negative swings exactly coincide with the two negative peak values at 4700 and 1400 m in Fig. 9 indicating that excursions outside the Category II ILS limit are due to the lateral acceleration errors. The INS-Kalman filter also had an excursion outside the Category II ILS limit at about 1400 m and

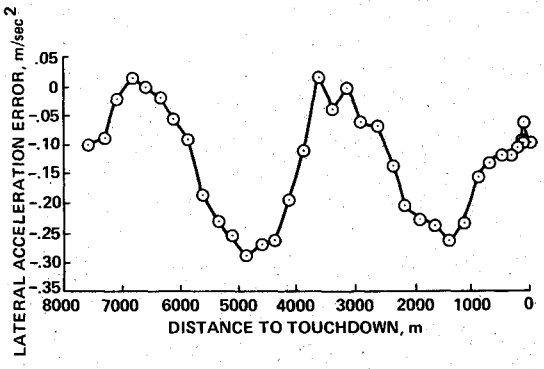

Fig. 9 Lateral acceleration error as a function of distance to touchdown.

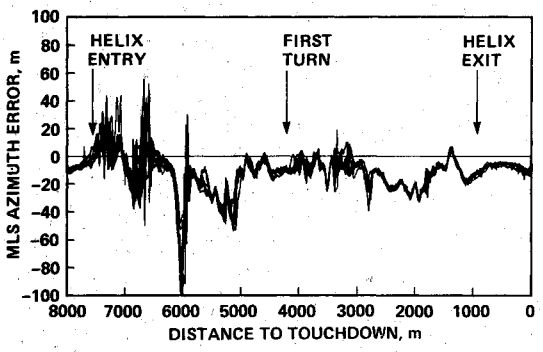

Fig.11 Composite plot from 14 flights, with angular MLS azimuth error multiplied by range to MLS azimuth transmitter.

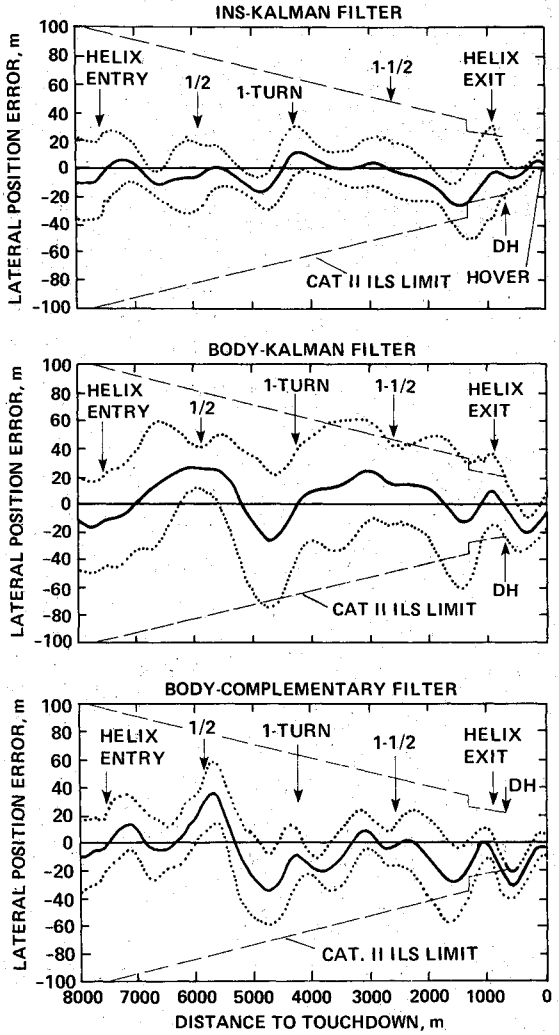

Fig. 10 Two-sigma lateral position error envelopes plotted about the mean for the first three navigation systems as functions of distance to touchdown.

a smaller excursion at 4700 m. These excursions are seen in this figure because the guidance system used the erroneous attitudes from the gyros instead of the INS to compute its commands. The lateral position error is the sum of the resulting guidance error and the Kalman filter estimation error.

Figure 10 also shows the effect of using fixed random forcing-function terms to compensate for different levels of inertial system quality. These terms were selected for best touchdown performance. For the body-Kalman filter, this resulted in good touchdown performance but poor tracking in the helix because too little weight was given to the MLS measurements. The best touchdown performance gains for the body-complementary filter resulted in better tracking in the helix than the body-Kalman system, but touchdown performance was always poorer. In the single flight with the fourth system, the INS-complementary filter system, the pilot reported that the helix tracking performance lay about halfway between that of the body-complementary and the INS-Kalman and that roll control activity was less than the body-complementary. This was consistent with the pilot reports that roll-control activity in the helix was always greatest with the body-complementary filter and least with the INS-Kalman filter.

During the letdown from hover to touchdown, some side-to-side and fore-and-aft motion was encountered with all navigation implementations. The INS-Kalman filter minimized these motions; the body-Kalman filter system was slightly worse. Although the pilots found this motion undesirable, they allowed all the body-Kalman and INS-Kalman filter system approaches to terminate at touchdown automatically. With the two complementary-filter system approaches, however, only a few were allowed to touch down automatically; more than half the approaches were terminated during the letdown by the pilot because of aft and sideward drift rates considered to be too high for a safe touchdown.

MLS Azimuth Errors

In an attempt to determine the cause of the long-period oscillations evident in Fig. 10 and the bias evident in Fig. 6, the MLS azimuth signal was examined in detail. Figure 11 shows a composite plot from 14 flights in which the angular MLS azimuth error has been multiplied by the range to the MLS azimuth transmitter.The angular MLS error is the difference between the MLS azimuth angle output from the MLS on-board receiver and the corresponding angle computed from the tracking radar data. The MLS azimuth error is plotted as a function of distance to touchdown along the runway center. This figure shows considerable noise in the received MLS signal, starting as the helicopter rolls into the turn and increasing rapidly during the first half turn, an indication of poor signal strength. Just before the half turn point, a large error spike of about -100 m occurs, caused by switching reception from the forward antenna to the rear antenna. A second but smaller spike occurs on the second turn. In both cases, following the spike, there is an erratic increase in error until about the three-quarter and one-and-three-quarter turn points, where the forward antenna is selected again. It is also clear that the noise is reduced as the helicopter descends and that a bias of about -10 m is present throughout the approach. Also, this figure shows a high degree of repeatability, indicating a very stationary MLS azimuth signal pattern.

The effect of the large spike at about 6000 m can be seen in Fig. 10, and the effectiveness of the "bad data" rejection scheme can be judged. The largest effect is on the body-complementary filter, which has a ±10 deg change limit on the MLS azimuth, feeding into a prefilter. The Kalman filter rejects the MLS azimuth data if the change exceeds four times the estimated error derived from the covariance matrix, which is larger for the body-mounted inertial system because of its larger inherent acceleration errors.

Conclusions

The following conclusions are based on the results of an initial flight test program of 49 automatic helix approaches, in which a reference radar tracking system was used that had 2-σ errors in x of 3.7 m (12 ft) and in y and z of 1.2 m (4 ft).

1) The research avionics system was capable of flying the helicopter along a precise helix flight path at 60 knots within a square area of approximately 1.2 km to a side.

2) Roll control activity in the helix was least with the Kalman filter systems. The pilot reported that the control activity of the INS-complementary flight was less than that of the body-complementary flights.

3) Tracking performance in the helix was best with the INS-Kalman filter. The performance of the INS-complementary flight was about midway between that of the INS-Kalman and the body-complementary. The body-Kalman filter gave the poorest tracking performance because of greater sensitivity to lateral acceleration errors.

4) Hover position precision was satisfactory, even though the CTOL Category II decision-height window dispersions were not met. Thus, the CTOL Category II decision-height tracking requirements may be too stringent for rotorcraft.

5) Both Kalman filters allowed fully automatic touchdowns on all approaches. The INS-complementary flight and most of the body-complementary flights were not allowed to touch down by the pilots because of excessive sideways drift and fore-and-aft drift.

6) The quality of the MLS azimuth angle output from the onboard receiver is degraded while the helicopter is in the helix because of antenna switching and a reduction in signal strength.

7) The transmitted MLS signal had a 0.2 deg bias that caused the position and navigation errors to be shifted 8 m to the left in the figures.

8) This flight test shows that the Kalman filter systems have the greatest potential for fully automatic approach and landing; however, all four techniques could deliver the aircraft to a hover over the landing pad at which point the pilot could perform the landing.

Recommendations for Further Study

The results of this flight test program demonstrate the need for further study. Three future study areas are identified:

1) Investigate methods to reduce the acceleration-error-generation process in the body-mounted inertial system. This would be particularly helpful in the body-Kalman approach.

2) Continue experiments with new MLS receiving antenna types. Recent results show potential for substantial noise reduction at the MLS receiver output.

3) Investigate the use of variable-gain complementary filter techniques for improved navigation performance, particularly in the vicinity of the landing pad.

References

[1]Hoffman, W.C., Hollister, W.M., and Howell, J.D., "Navigation and Guidance Requirements for Commercial VTOL Operations," NASA CR-132423, 1974.

[2]Liden, S., "V/STOLAND Digital Avionics System for UH-1H," Final Report, NASA CR-152179, 1979.

[3]Schmidt, S.F. and Mohr, R.L., "Navigation Systems for Approach and Landing of VTOL Aircraft," NASA CR-152335, 1979.

[4]Foster, J.D., McGee, L.A., and Dugan, D.C., "Helical Automatic Approaches of Helicopters with Microwave Landing Systems," NASA TP-2109, 1982.

[5]"Heliport Design Guide," Advisory Circular No. 150-5390, Dept. of Transportation, Federal Aviation Administration, Aug. 1977.

[6]"Criteria for Approving Category I and Category II Landing Minima for FAR 121 Operations," Advisory Circular No. 120-29, Dept. of Transportation, Federal Aviation Administration, Washington, D.C., 1970.